Influence of a $SiO_2-CaO-P_2O_5$ Sol−Gel Glass on the Bioactivity and Controlled Release of Ceramic/Polymer/Antibiotic Mixed Materials

D. Arcos, J. Peña, and M. Vallet-Regí*

Departamento de Química Inorgánica y Bioinorgánica, Facultad Farmacia, Universidad Complutense de Madrid, Madrid, Spain

Received April 14, 2003. Revised Manuscript Received July 3, 2003

Materials based on ceramic−polymer−gentamicine blends with potential application as prefabricated bone blocks and drug delivery systems have been synthesized. Three series of materials have been prepared with varying composition of the ceramic fraction. The ceramic component of series S1 contains only hydroxiapatite (HA), series S2 contains HA and 2.7% sol−gel glass, and series S3 contains 29% glass. Series S3 develops an apatite-like phase on the surface when soaked in simulated body fluid (SBF). Series S2 undergoes surface changes, but the development of an apatite-like phase does not occur. Finally, series S1 does not exhibit significant changes at the surface. Materials with 29% glass show an important surface area reduction during the first 24 h due to the formation of an amorphous calcium phosphate before the OHAp crystallization. This surface reduction leads to a retardation of the drug release during this period compared to the samples with no glass or 2.7% glass. The results presented in this work point out that when synthesizing bioactive materials to be used as drug delivery systems, the important surface modifications must be considered for the drug release kinetics.

Introduction

The study and development of materials for bone filling and replacement is one of the most important fields in orthopedic surgery. Among these materials some ceramics, called bioactive ceramics, have shown an excellent behavior when in contact with living bone.[1−3] These materials lead to the integration of the bone tissue with the implant, promoting the bone regeneration and successful healing of the tissue. However, there is an important drawback associated with the implantation of bone blocks and fillers: the risk of infection often leads to high osteomielitis incidence.[4,5] Systemic antibiotic administration is usually applied, but poor blood circulation in the bone is the main cause of a reduced therapeutic effect.

Local drug release seems to be a very promising alternative. Obtaining bioactive implants able to locally deliver drug would be an added value to these implants, and several attempts have been made in this sense.[6−8] One possible alternative is to synthesize ceramic/polymer composites loaded with a wide spectrum antibiotic. The polymeric matrix would control the drug release, while the ceramic fraction would ensure the bone integration with the implant.[9−15]

Two of the most important bioactive ceramics are synthetic hydroxiapatite (HA) and bioactive glasses. HA has been used as a bioactive ceramic since the early 1970s, showing excellent biocompatibility. This ceramic is able to join bone tissue through a bioactive bond; however, this bonding process takes a long time, when compared to that of the glasses.[16,17] In this sense, the degree of crystallinity seems to have a very important influence.[18] Several authors have reported that bioactive glasses undergo an intense surface reaction when

* To whom correspondence should be addressed. E-mail: vallet@farm.ucm.es.

(1) Hench, L. L.; Wilson, J. *An Introduction to Bioceramics*; Advanced Series in Ceramics; World Scientific: Singapore, 1995; Vol. 1, p 1.
(2) Hench, L. L. *J. Am. Ceram. Soc.* **1991**, *74*, 1487.
(3) Vallet-Regí, M. *J. Chem. Soc., Dalton Trans.* **2000**, 97.
(4) Oga, M.; Sugioka, Y.; Hobgood, C. D.; Gristina, A. G.; Myrvik, Q. N. *Biomaterials* **1988**, *9*, 285.
(5) Bucholz, H. W.; Heinet, K.; Foerster, G. W. In *Orthopaedic Infections*; D'Ambrosia, R.D., Marier, R.L., Eds.; Slack, Inc.: Thorofare, NJ, 1989; pp 477−488.
(6) Kawanabe, K.; Okada, Y.; Matsune, Y.; Lide, H.; Nakamura, T. *J. Bone Joint Surg.*, **1998**, *80-B*, 527.
(7) Itokazu, M.; Sugiyama, T.; Ohno, T.; Wada. E.; Katagiri, Y. *J. Biomed. Mater. Res.* **1997**, *39*, 536.
(8) Meseguer-Olmo, L.; Ros-Nicolás, M. J.; Clavel-Sainz, M.; Vicente-Ortega, V.; Alcaraz-Baños, M.; Lax-Pérez, A.; Arcos, D.; Ragel, C. V.; Vallet-Regí, M. *J. Biomed. Mater. Res.* **2001**, *61*, 458.
(9) Arcos, D.; Ragel, C. V.; Vallet-Regí, M. *Biomaterials* **2001**, *22*, 701.
(10) Del Real, R. P.; Padilla, S.; Vallet-Regí, M. *J. Biomed. Mater. Res.* **2000**, *52*, 1.
(11) Ragel, C. V.; Vallet-Regí, M. *J. Biomed. Mater. Res.* **2000**, *51*, 424.
(12) Padilla, S.; del Real, R. P.; Vallet-Regí, M. *J. Controlled Release* **2002**, *83*, 343.
(13) Vallet-Regí, M.; Gordo, M.; Ragel, C. V.; Cabañas, M. V.; San Román, J. *Solid State Ionics* **1997**, *101−103*, 887.
(14) Arcos, D.; Cabañas, M. V.; Ragel, C. V.; Vallet-Regí, M.; San Román, J. *Biomaterials* **1997**, *18*, 1235.
(15) Granado, S.; Ragel, V.: Cabañas, V.; San Román, J.; Vallet-Regí, M. *J. Mater. Chem.* **1997**, *7*, 1581.
(16) Oonishi, H.; Hench, L. L.; Wilson, J.; Sugihora, F.; Tsuji, E.; Matsuura, M.; Kin, S.; Yamamoto, T.; Mizokawa, S. *J. Biomed. Mater. Res.* **2000**, *51*, 37.
(17) Ducheine, P.; Qiu, Q. *Biomaterials* **1999**, *20*, 2287.
(18) Shi, D. L.; Jiang, G. W.; Bauer, J. *J. Biomed. Mater. Res.* **2002**, *63*, 71.

10.1021/cm031074n CCC: $25.00
Published on Web 09/23/2003

treated with simulated body solutions under in vitro conditions,[19−21] whereas the ceramic HAs are more stable under the same conditions.

Actually, bioactive glasses bond to bone through the formation of a new apatite-like phase at the surface.[22] This process is the result of an ionic exchange between the glass and the environment when the implant gets in contact with physiological fluids. Afterward, the glass develops a silica rich layer at the surface that facilitates the nucleation of an apatite phase taking Ca^{2+} and phosphates from the fluids.[23] Recent works have shown that by incorporating a portion of bioactive glass to HA pieces, the bioactive behavior improves significantly, leading to a thicker new HCA layer on the surfaces when compared to that obtained with the glass alone.[24−26]

The idea of incorporating bioactive materials into acrylic cements, to ensure a good osteointegration, has been developed by different authors.[27−29] Moreover, acrylic matrixes such as PMMA have been used since the 1970s for drug delivery.[30] However, no studies about the influence of the bioactive process on drug diffusion kinetics have been done. Because bioactivity is a surface effect, the drug diffusion kinetic must be affected. This fact should become more evident when the ceramic component is especially reactive, like bioactive glasses.

In this work we have synthesized materials formed by a hydrophobic polymeric matrix (PMMA), a ceramic component, and a drug. The PMMA allows the controlled release of the drug, and the ceramic component should supply the bioactive behavior to the system. The ceramic fraction is composed by two phases: hydroxyapatite (HA) and a bioactive sol−gel glass, with the final aim of this work being to study the role of the glass in the behavior of these blends in terms of bioactivity and drug release. The drug is gentamicine sulfate, a wide spectrum antibiotic with action on bacteria that lead to osteomielitis, i.e., *Staphylococcus aureus* and *Streptococcus* spp.

Experimental Section

Synthesis of Hydroxyapatite (OHAp). The OHAp was synthesized by the precipitation method from $Ca(NO_3)_2{\cdot}4H_2O$ 0.6 M and $(NH_4)_2HPO_4$ 1 M solutions. Both solutions were dropped into a reactor and were kept under stirring at 90 °C for 24 h, maintaining pH 10 by adding NH_3 solution. The product was washed with hot water to remove NH_3 and the nitrates. Subsequently, the product was dried at 100 °C, fired at 700 °C for 2 h, milled, and sieved. At this point, the material was no longer a gel, it had become a sol−gel glass. Particles ranging in size between 32 and 68 μm were collected.

Table 1. Experimental[a] and Theoretical Compositions (wt %)

	OHAp	S58	PMMA	Gentamicine
S1 experimental	36.30		54.50	9.20
S1 theoretical	52.00		35.00	13.10
S2 experimental	34.50	1.80	54.50	9.20
S2 theoretical	51.30	2.70	32.30	13.70
S3 experimental	18.15	18.15	54.50	9.20
S3 theoretical	29.00	29.00	29.00	13.00

[a] Experimental values are those referred to the real polymer content and considering that the mass of HA, glass, and gentamicine are not affected during the polymerization process.

Synthesis of the Sol−Gel Glass (58S). A glass of nominal composition 58:36:6 (% mol) $SiO_2/CaO/P_2O_5$ has been synthesized by hydrolysis and polycondensation of tetraethylorthosilane (TEOS), triethyl phosphate (TEP), and $Ca(NO_3)_2{\cdot}4H_2O$. To catalyze the reagent hydrolysis, a 2 N solution of HNO_3 was added. The reagents ratio for the hydrolysis process was [mol H_2O/(mol TEOS + mol TEP)] = 8. The TEP and calcium nitrate were successively added to the TEOS−H_2O−HNO_3 mixture under stirring, with 1-hour intervals between consecutive additions. After mixing all the reagents, the solutions were placed in closed Teflon jars, where the gelation process took place at room temperature. These gels were aged at 70 °C for 3 days and dried at 150 °C for 52 h after replacing the lids with new ones with a 1-mm hole. The dried gels were stabilized at 700 °C for 3 h and then milled and sieved, choosing the powders with sizes ranging from 32 to 68 μm.

Synthesis of the Ceramic/Polymer/Antibiotic Blends. We have synthesized three series of mixed materials. The compositions are provided in Table 1. We have kept constant the ceramic/polymer/gentamicine ratio, although the ceramic fraction is different from one series to each other. The ceramic fraction of S1 materials contains OHAp as the only ceramic phase, whereas S2 and S3 contain 5% and 50% of sol−gel glass, respectively. The experimental procedure can be described as follows. OHAp and glass were mixed using a vibrating ball mill for 6 h. Afterward, the gentamicine sulfate was incorporated into the ceramic mixture and finely dispersed by an additional mixing process. Separately, a solution of polymethyl methacrylate (PMMA) and methyl metacrylate (MMA) was prepared. The polymer/monomer ratio was 1:2 and 0.5% of benzoil peroxide was added as initiator of the polymerization reaction. The OHAp/glass/gentamicine mixture was incorporated into the PMMA−MMA solution. The resulting paste was homogenized in an ultrasonic bath for 15 min and poured into Teflon molds. The polymerization took place in 24 h at 60 °C, obtaining solid pieces of dimensions 8 × 8 × 4 mm. Gentamicine sulfate melts at 244 °C and decomposes at 330 °C. Under this experimental conditions (0.5% benzoyl peroxide and 60 °C), we can expect only a small temperature increase depending on the MMA mass, and this temperature rise should not affect this drug. TG/DTA analysis were made with inner and outer parts of the pieces, showing that ceramic, drug and polymer were homogeneously distributed. No abrading was carried out on the sample surfaces. Table 1 collects the theoretical values as well as the experimental results obtained by thermogravimetrical analysis (TGA). These data show that the amount of PMMA is around 25% lower compared with the theoretical ones, due to the partial loss of MMA during polymerization.

In vitro Testing. To test the in vitro bioactivity and the drug release, the samples were soaked in 50 mL of simulated body fluid (SBF),[31] which contains an ionic composition similar

(19) Peltola, T.; Jokinen, M.; Rahiala, H.; Levänen, E.; Rosenholm, J. B.; Kangasniemi, I.; Yli-Urpo, A. *J. Biomed. Mater. Res.* **1999**, *44*, 12.
(20) Pereira, M. M.; Clark, A. E.; Hench, L. L. *J. Biomed. Mater. Res.* **1994**, *28*, 693.
(21) Vallet-Regí, M.; Arcos, D.; Pérez-Pariente, J. *J. Biomed. Mater. Res.* **2000**, *51*, 23.
(22) Hench, L. L.; Wilson, J. *Science* **1984**, *226*, 630.
(23) Hench, L. L.; Andersson, O. Bioactive Glasses. In *An Introduction to Bioceramics*; Hench, L. L., Wilson, J., Eds.; World Scientific Publishing: Singapore, 1993; p 41.
(24) Ragel, C. V.; Vallet-Regí, M.; Rodriguez-Lorenzo, L. M. *Biometerials* **2002**, *23*, 1865.
(25) Rámila, A.; Padilla, S.; Muñoz, B.; Vallet-Regí, M. *Chem. Mater.* **2002**, *14*, 2439.
(26) Vallet-Regí, M.; Rámila, A.; Padilla, S.; Muñoz, B. *J. Biomed. Mater. Res.* **2003**, *66A*, 580.
(27) Miyaji, F.; Morita, Y.; Kokubo, T.; Nakamura, T. *J. Ceram. Soc. Jpn.* **1998**, *106*, 465.
(28) Shinzato, S.; Kobayashi, M.; Mousa, W. F.; Kamimura, M.; Neo, M.; Kitamura, Y.; Kokubo, T.; Nakamura, T. *J. Biomed. Mater. Res.* **2000**, *51*, 258.
(29) Dalby, M. J.; Di Silvio, J.; Harper, E. J.; Bonfield, W. *Biomaterials* **2001**, *22*, 1739.
(30) Wahlig, H.; Dingeldein, E.; Bergmann, R.; Reuss, K. *J. Bone Jt. Surg. Br.* **1978**, *60-B*, 270.
(31) Kokubo, T.; Kushitani, H.; Sakka, S.; Kitsugi, T.; Yamamuro, T. *J. Biomed. Mater. Res.* **1990**, *24*, 721.

to that of human plasma. The soaked samples were maintained at 37 °C for 15 days. The calcium solubility test and pH evolution were carried out using an Ilyte Na^+, K^+, Ca^{2+}, pH system. The surface morphology was studied by scanning electron microscopy (SEM) using a JEOL 6400-LINK IN AN 1000 microscope.

The gentamicine released was determined as a function of soaking time. Measurements were carried out by means of UV−Vis spectroscopy with a Beckman DU-7 spectrophotometer using the *o*-phthaldialdehyde method.[32] Absorbance values were taken at a wavelength $\lambda = 331$ nm, at which the gentamicine−phthaldialdehyde complex shows an absorbance maximum. To obtain statistically significant data, seven samples of each series were studied. The absorbance reading was taken five times for each measurement, and the arithmetic mean was calculated.

The N_2 adsorption isotherms were obtained using a Micromeritics ASAP 2010C instrument. To perform the N_2 adsorption measurements, the samples were first outgassed for 24 h at 25 °C. The surface area (S_{BET}) was determined using the Brunauer−Emmett−Teller (BET) method.[33] The pore size distribution between 1.7 and 130 nm was determined from the desorption branch of the isotherm by means of the Barret−Joyner−Halenda (BJH) method.[34]

Results

Figure 1a shows the Ca^{2+} release from the samples when they are soaked in SBF. The calcium content of SBF does not change when S1 materials are soaked. For S2 there is a small Ca^{2+} increase from 87 to 95 ppm during the first 24 h, remaining constant until the end of the test. Ca^{2+} content for S3 shows a higher increase from 87 to 104 ppm during the first 24 h of test. Afterward, the Ca^{2+} content clearly decreases, falling to values of 83 ppm at the end of the test.

Figure 1b shows the pH evolution in the SBF as a function of time. When S1 materials are soaked, very small (negligible) variation is observed. Soaking of the S2 blend leads to a very small pH increase, from 7.2 to 7.35 during the first 24 h, remaining constant until the end of the test. However, S3 blends lead to a clear pH increase during the first 2 days, reaching pH values of 7.9−8.0, and remaining constant until the end of the test.

Finally, Figure 1c shows the P and Si concentration for series S3. The P release profile shows a small increase during the first hours. After 6 h, P concentration in SBF decreases, pointing out that a precipitation process is taking place. The Si concentration increased in SBF during the first 72 h, remaining constant until the end of the test. These data point out that the glass undergoes a partial dissolution, following the mechanism described for the bioactivity in silicon-based glasses.[23] Series S1 and S2 do not show significant changes of the Si or P concentration during the test, remaining close to the original values (before soaking).

Figure 2 shows the N_2 adsorption isotherms for the materials studied. Samples S1 and S2 show type II isotherms, characteristic of materials with low porosity and, in our case, low surface area. The S3 curve can be identified as a type IV isotherm characteristic of a material containing mesopores, showing an H1 type hysteresis loop in the mesopore range.

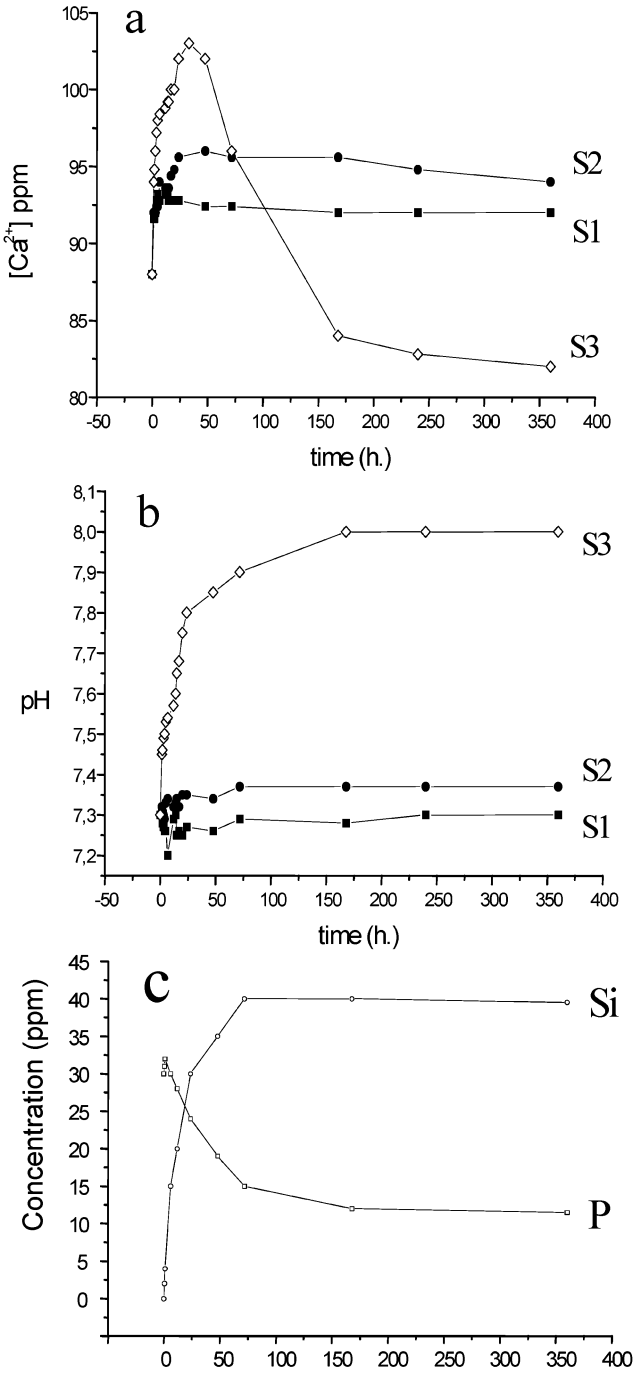

Figure 1. SBF chemical changes as a function of blends soaking time: (a) Ca^{2+} concentration, (b) pH evolution and (c) P and Si concentration for series S3.

Table 2 shows the surface area and pore volume of the blends before and after being soaked for 1 and 15 days. As it can be seen S3 blends have the highest surface area before soaking, due to the highest content in sol−gel glass. After 1 and 15 days soaking in SBF, the surface area and pore volume of S1 and S2 series do not change significantly. In contrast, S3 mixture shows a significant decrease in S_{BET} and pore volume after 1 day, partially recovering the values after 15 days in SBF.

Figure 3 shows the pore size distribution before and after soaking the pieces in SBF. S1 mixed materials

(32) Sampth, S. S.; Robinson, D. H. *J. Pharm. Sci.* **1990**, *79*, 428.
(33) Gregg, S. J.; Sing, K. S. W. *Adsorption, Surface Area and Porosity*, 2nd ed.; Academic Press: New York, 1982; p 57.
(34) Barret, E. P.; Joyner, L. J.; Halenda, P. P. *J. Am. Chem. Soc.* **1951**, *73*, 373.

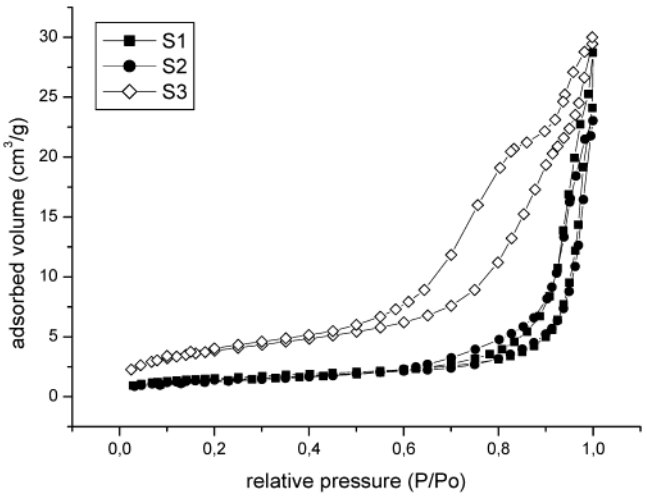

Figure 2. N_2 adsorption isotherms of S1, S2, and S3.

Table 2. Surface Area and Pore Volume of the Materials Before and After Being Immersed in SBF for 1 and 15 days

	surface area [m^2/g]	pore volume [cm^3/g]
S1	5.5	0.044
S1−1d	5.2	0.039
S1−15d	6.6	0.037
S2	5.0	0.035
S2−1d	7.1	0.032
S2−15d	6.2	0.032
S3	13.9	0.046
S3−1d	3.4	0.019
S3−15d	8.8	0.034

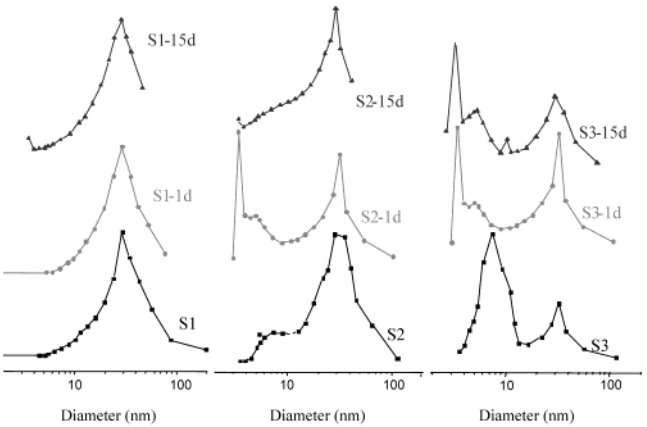

Figure 3. Pore size distribution of S1, S2, and S3 before (0 days) and after being soaked in SBF; the *y* axis represents *dV*/*d*log(D).

show a single modal distribution, centered at the mesopore region on 33 nm. The HA component shows the same distribution when measured alone, and PMMA does not show porosity at this region. So we can admit that this porosity is provided by the HA component. After 1 and 15 days, the textural properties did not change, maintaining the same porosity, surface area, and pore diameter as shown in Table 2.

S2 blends show the same distribution centered at 33 nm, together with a shoulder centered between 5 and 12 nm. Taking into account that 58S glass alone shows a pore size distribution into this range,[35] the second small distribution can be assigned to the small amount of glass contained in this sample. After 1 day in SBF, the pore size distribution changes. The shoulder corresponding to the glass disappears, whereas a new sharp distribution centered at 3−4.5 nm and a small maximum centered at 5−6 nm appear. On the other hand, the distribution attributable to HA remains the same. After 15 days, the textural properties are similar to the initial situation although the shoulder corresponding to the glass does not appear.

S3 mixed materials show, before soaking, a bimodal pore size distribution centered at 33 and 8 nm, corresponding to the mesoporosity supplied by the HA and glass component, respectively. After 1 day in SBF, the distribution corresponding to the glass disappears, showing a pore size distribution similar to that observed in S2 blends after 1 day of soaking: two new distributions centered at 5 nm and a sharper one at 3.5 nm. After 15 days, these two pore distributions remain at the surface of the sample. Moreover, another one appears with a maximum centered at 10.5 nm.

Figure 4 collects the micrographs obtained for S3 mixtures before and after being soaked in SBF. The surface of the S3 mixed materials is formed by particles of irregular shape, leaving large macropores with sizes as large as 50 μm. After 1 day in SBF, the surface morphology does not change. The higher magnification of this micrograph allows observation of the big polymer particles interconnected and forming such large macropores. After 3 days, the surface morphology clearly changes. A new phase has grown onto the material, covering the macropores observed before and after 1 day of soaking. This new layer is stable after 15 days, reaching a thickness of 1−1.5 μm as can be seen in Figure 5. EDX experiments confirmed that this new layer is mainly composed of Ca and P, indicating that a calcium phosphate layer has grown by taking Ca^{2+} and PO_4^{3-} from the SBF. In other words, samples S1 and S2 show surface morphology similar to that of S3 before soaking. No significant changes were observed for these two samples during the study.

Drug Release Test. The gentamicine release study was carried out by soaking pieces of 8 × 8 × 4 mm and 300 mg of weight, into 50 mL of SBF. Figure 6 shows the gentamicine sulfate released as a function of soaking time for S1, S2, and S3 mixed materials. During the first 5 h, the three series show a very similar behavior, releasing 40 wt % of the drug content. After 6 h S1 and S2 do not show significant differences, releasing 70% of the drug after 9−10 h and 80% after 14 h. Afterward, the drug release occurs at a slower pace, releasing 90% after 48 h.

S3 blend shows a more controlled drug release at the time interval between 6 and 24 h. After 9 h, less than 60% is released, and 20 h is required to liberate 80% of the drug.

For the study of the gentamicine release kinetics, the fraction of gentamicin released versus the square root of time can be fitted to a third-order polynomial, corresponding with the model proposed by Cobby et al.[36] for this kind of system (insoluble matrix − partially in

(35) Balas, F.; Arcos, D.; Pérez-Pariente, J.; Vallet-Regí, M. *J. Mater. Res.* **2001**, *16*, 1345.

(36) Cobby, J.; Mayerson, M.; Walker, G. C. *J. Pharm. Sci.* **1974**, *63*, 725.

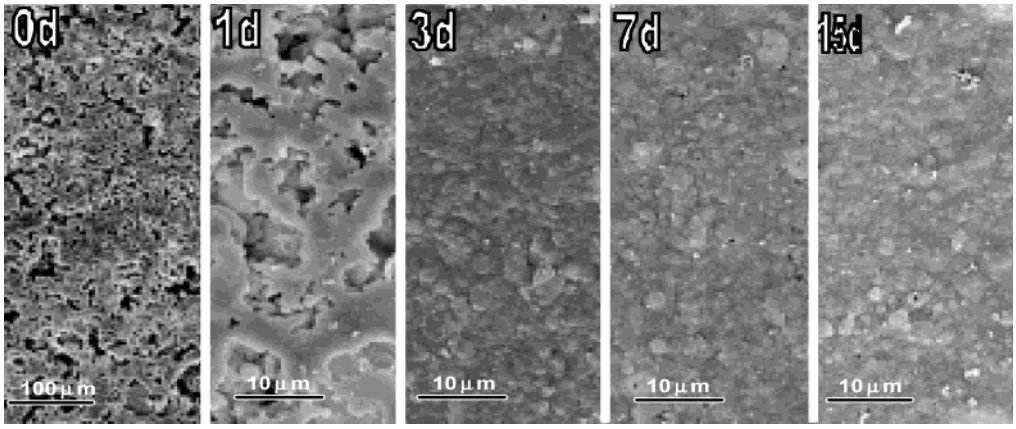

Figure 4. SEM micrographs of S3 materials before (0 days) and after being soaked in SBF. S1 and S2 before and after soaking show morphology similar to that of S3 composites before soaking.

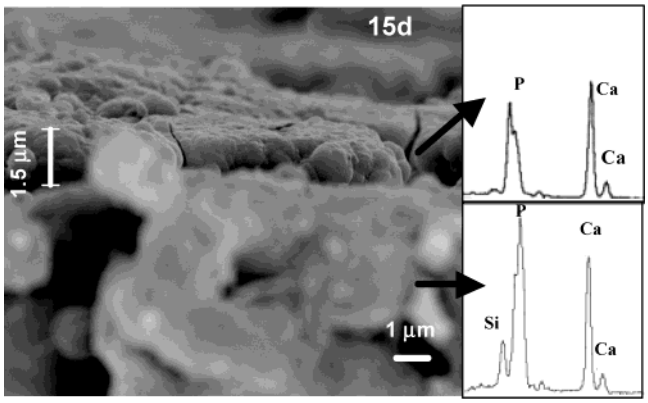

Figure 5. Cross section of a S3 piece after 15 days in SBF. A newly formed layer is clearly seen over the material surface. EDX analysis showed that this layer is formed by Ca and P.

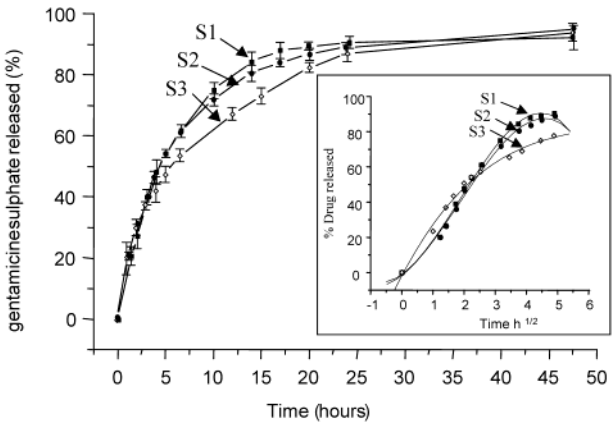

Figure 6. Gentamicine release as a function of soaking time for S1, S2, and S3. Inset: gentamicine released as a function of square root of time. The fit to a third-order polynomial function is also plotted.

this case − with pores and canals, and parallelepiped−shaped with all the surfaces exposed to the medium).

The equation that described this behavior is

$$f_t = \frac{(a_0b_0 + a_0b_0 + b_0c_0)}{V_0} K_b t^{1/2} - \frac{(a_0 + b_0 + c_0)}{V_0} K_b{}^2 t + \frac{1}{V_0} K_b{}^3 t^{3/2}$$

where f_t is the fraction of drug released at time (t) and K_b is the boundary retreat rate constant. This constant is a measure of the rate at which dissolution fluid is able to penetrate into the matrix to effect drug dissolution and release. The parameters a_0, b_0, and c_0 are the parallelepiped dimensions, and V_0 is the parallelepiped volume. The complexity of the materials presented in this work introduces some differences with respect to those reported by Cobby. However, in general terms, the drug is introduced into the matrix in a way similar to that used by this author: mixed in a liquid phase and left to harden. The final result is that one fraction of the drug is embedded in the PMMA matrix and another (in our case) is intercalated macroscopically between the ceramic particles.

The K_b values obtained from fitting the experimental values to the equation are

$$K_b(\mathrm{S1}) = 0.482\ \mathrm{mm{\cdot}h^{-1/2}}\ (\pm 0.02)$$

$$K_b(\mathrm{S2}) = 0.480\ \mathrm{mm{\cdot}h^{-1/2}}\ (\pm 0.03)$$

$$K_b(\mathrm{S3}) = 0.360\ \mathrm{mm{\cdot}h^{-1/2}}\ (\pm 0.03)$$

In biomaterials science, we must take into account that each bone defect requires a different implant shape. The Cobby model provides constants that are independent of the matrix shape (not dimensions). Therefore, the K_b values calculated in this work would be the same for cylindrical, spherical, or biconvex implants for determined radius dimensions.

Discussion

In recent works, the synergic effect on bioactivity of sol−gel glasses with hydroxyapatite has been shown.[24−26] Actually, OHAp does not show in vitro bioactivity; i.e., it does not develop a new apatite phase when soaked in SBF or other simulated body fluids. However, Vallet-Regi et al. reported that the combination of OHAp with a small amount (5%) of sol−gel glass leads to the formation of a newly grown apatite layer, even thicker than that formed on glasses alone.

The polymer−ceramic materials obtained in this work contain OHAp (S1) and two mixtures of glass−OHAp (S2 and S3) as ceramic fraction. By using the combination glass−OHAp, we pretended to obtain materials with higher bioactivity, and to study the consequences

of the surface changes on the release of the drug. Moreover, by introducing two different glass percentages against the amount of OHAp, 5 and 50% for S2 and S3, respectively, we deal with two possibilities: (1) a small amount of glass mixed with OHAp is enough to show in vitro bioactivity, or (2) higher amounts of sol−gel glass are required.

Ca^{2+} and pH measurements evidence differences in the ionic exchange between different samples. Samples of S3 show the highest degree of ionic exchange. Sample S2 also showed this process but in a much lower degree, whereas sample S1 does not show it. The exchange between Ca^{2+} from the glass and H^+ from the fluid leads to pH increase, Ca^{2+} saturation, and Si−OH formation on the glass surface. These processes are necessary for the subsequent development of an apatite-like phase on the glass surface.[23] Obviously, the higher amount of glass in samples S3 enhances this reactions.

The mechanism proposed by Hench[23] establishes that after formation and polycondensation of the Si−OH groups, an amorphous calcium phosphate (ACP) grows on the surface, taking Ca^{2+} and PO_4^{3-} from the fluid. Afterward, this ACP crystallizes into an apatite phase. Because this process takes place on the surface, the textural properties of the materials must reflect the consequences of these changes. Actually, before soaking, the three materials show pore size distributions which are a consequence of the addition of the individual porosities of the glass and the OHAp. In this sense, sample S1 shows the distribution corresponding to OHAp, S2 shows mainly the same distribution together with a small shoulder assignable to the glass, and S3 clearly shows the contributions of glass and OHAp. In addition, the higher the glass content, the higher the surface area. The evolution of the textural properties as a function of soaking time seems to agree with the different degree of ionic exchange observed. Samples S1 do not undergo significant surface area (S_{BET}) or pore volume (PV) reduction with soaking time, and the pore-size distribution does not change. Likewise, S2 samples do not show considerable changes in either S_{BET} or PV values. However, after 1 day, the small ionic exchange observed in Figure 1 leads to modifications in the pore size distribution. A new distribution appears around 4 nm, but after 15 days only OHAp distribution remains. These data point out that the small amount of glass in S2 leads to an initial reaction, but there is not enough glass to develop a new phase at the surface. Moreover, after 15 days the small amount of glass seems to be dissolved, as it is indicated by the absence of the shoulder corresponding to the glass pore size distribution. It is well-known that during the bioactive process the silicon network is partially degraded into soluble $Si(OH)_4$.[37]

In agreement with the ionic exchange results, S3 materials show important changes at the surface. After 1 day in SBF, an important decrease of S_{BET} and PV occurs. This fact is coincident with the substitution of the glass pore size distribution by a new one, similar to that observed in S2 samples after 1 day. After 15 days, the S_{BET} and PV are partially restored and the pore size distribution points out that a new phase has grown on the surface. The SEM micrographs confirm this point. Actually, only S3 sample shows the typical surface morphology of an apatite-like phase grown on the surface of bioactive materials.

These results point out that, in these blends, a small presence of glass together with OHAp is not enough to develop a new apatite phase (blend S2). The biphasic materials obtained in refs 24−26 contained only sol−gel glass and OHAp and showed an excellent bioactive behavior. The authors explained that such a small amount of glass is enough to trigger the bioactive process, whereas OHAp acts as a good seed to induce the growth of the new phase. However, the materials presented in this work also contain an hydrophobic acrylic polymer (PMMA). The initial ionic exchange with the fluid is lowered and an important fraction of glass and OHAp is covered by the polymer. Consequently, the small amount of glass contained in samples S2 is not enough to show bioactivity. Pore size evolution of S2 shows that there is an initial reaction of the glass component, leading to temporal surface changes. However, it does not evolve toward a new apatite phase, but only to the glass dissolution at the material surface.

Samples S3 not only suffer modifications of their surface during the first 24 h, but also develop a new apatite-like layer as can be seen in SEM micrographs. As expected, samples without sol−gel glass (blends S1) do not show bioactive behavior. These results point out that in blends composed by OHAp−glass−PMMA there is no synergic effect between OHAp and the glass. The hydrophobic nature of the PMMA makes difficult the interaction between the sample and the SBF. Moreover, the polymer probably covers the glass and the OHAp particles, therefore the glass activity is reduced and the OHAp particles cannot act as seeds for the new apatite phase nucleation. In this case, the glass seems to be the only material responsible for the bioactive behavior, so the higher the glass content the better the bioactive response.

When we use bioactive implants as drug delivery systems, the surface changes during the bioactive process must be taken into account. The results presented in this work prove that, when the bioactive process is intense enough, the drug release kinetics is modified. Actually, samples S1 and S2 show almost identical release kinetics whereas the drug release is slowed in S3, exactly between 6 and 24 h. This fact is easily explained by the surface area reduction that S3 samples undergo during this period. Certainly, the differences observed between S3 samples and the others are not very great, however they are statistically significant (see error bars in Figure 6 and standard deviation of the boundary retreat rate constants).

We can conclude that a bioactive process takes place in the system OHAp/sol−gel glass/PMMA/gentamicine systems when the sol−gel glass amount is high enough. During this process, between 6 and 24 h, a surface area reduction occurs, decreasing the drug release during that period.

To understand the mechanism of such surface area decrease, and, consequently, the slower drug release, we need to know the changes produced on the surface during this period. For this purpose, we have followed the textural and chemical changes of the glass by N_2

(37) Arcos, D.; Greenspan, D. C.; Vallet-Regí, M. *Chem. Mater.* **2002**, *14*, 1515.

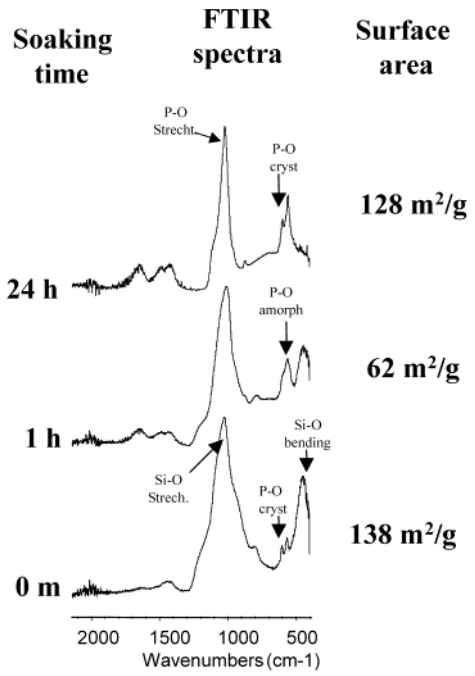

Figure 7. FTIR spectra and surface area of 58S sol−gel glass before and after being soaked in SBF for 1 h and 24 h.

adsorption and FTIR spectrometry when soaked in SBF. The study of the different stages of a CaP formation on the blends is very difficult because of the presence of the synthesized OHAp contained in the samples. The intense vibrations bands corresponding to the synthetic OHAp overlap the low intense bands corresponding to the new apatite layer formed on the surface. Moreover, the sol−gel glass is the component that provides bioactivity, and the component that undergoes the most important changes, as well. In fact, this experiment was carried out to elucidate the mechanism that causes the surface area diminution and, consequently, the drug release decrease during that period.

Figure 7 shows the FTIR spectra obtained using diffuse reflectance optic from the glass surface, as well as the surface area measured before and after 1 and 24 h of soaking in SBF. The glass before soaking shows the absorption bands corresponding to the different vibration modes of the Si−O bonds. A doublet at 580−610 cm^{-1} can also be observed. This doublet is characteristic of crystalline CaP and can be due to the presence of small CaP crystallites formed at the glass surface, as a consequence of the glass reactivity with the atmospheric water. At this point, the glass show a surface area of 138 m^2/g. After 1 h, the surface area drastically decreases to 62 m^2/g. This decrease is coincident with the appearance of a singlet at 600 cm^{-1}, which overlaps the doublet observed before soaking. This singlet corresponds to the formation of amorphous CaP that covers the glass surface and decreases the surface area of the material. Because only surface information is collected with the optic used in this experiment, only the bands corresponding to the new apatite layer grown on the surface can be seen after 24 h. The amorphous CaP turns into crystalline apatite, as is pointed out by the new doublet at 580−610 cm^{-1}. As can be seen, the crystallization process leads to partial restoration of the surface area values. These results indicate that the surface area reduction of the sol−gel glass during the bioactive process is produced by the amorphous CaP layer growth over the glass. When the glass alone is soaked in SBF, the minimum surface is reached after 1 h, whereas the blends need 24 h. This is easily explained by the much higher bioactivity of the glass when compared with the mixtures of OHAp−glass−PMMA−gentamicine. However, if the glass amount is high enough, the formation of amorphous CaP also occurs in the blends, leading to a temporal surface area reduction and decreasing the gentamicine release kinetics. Although the difference in drug release between sample S3 and samples S1 and S2 is not very high in this experiment, it must be taken into account when considering in vivo studies, where release times are longer. The drug release decrease (due to the amorphous CaP formation at the surface) cannot be considered as a method to achieve a more controlled release. However, it is a factor that must be considered for the use of bioactive implants as drug delivery systems.

Conclusions

(1) Mixtures of OHAp−PMMA−gentamicine and OHAp−Sol−gel glass−PMMA−gentamicine have been obtained. These materials have two simultaneous potential applications: bone replacement and drug delivery system. (2) The sol−gel glass determines the in vitro bioactivity of the blends. The higher the amount of glass, the better the in vitro bioactivity. (3) Small amounts of glass together with OHAp do not lead to in vitro bioactive materials. The presence of a hydrophobic acrylic polymer avoids the synergic effect of these components on the bioactive behavior. (4) Blends with a glass amount high enough to develop a new apatite phase undergo a surface area reduction between 6 and 24 h. This reduction is due to the formation of an amorphous CaP phase at the surface. The lower surface area leads to a decrease in the drug release kinetics. (5) The temporal S_{BET} reduction and, consequently, the drug release decrease, must be taken into account when using bioactive implants as drug delivery systems.

Acknowledgment. Financial support of CICYT, Spain, through research project MAT02-00025 is acknowledged. We also thank A. Rodriguez (Electron Microscopy Center, Complutense University) and F. Conde (C.A.I. X-ray Diffraction Centre, Complutense University), for valuable technical and professional assistance.

CM031074N